

Fluxes of Sedimentary Material in the Lofoten Basin of the Norwegian Sea: Seasonal Dynamics and the Role of Zooplankton

A. V. Drits^{a, *}, A. A. Klyuyvitkin^{a, **}, M. D. Kravchishina^a, V. A. Karmanov^b, and A. N. Novigatsky^a

^a*Shirshov Institute of Oceanology, Russian Academy of Sciences, Moscow, Russia*

^b*Lomonosov Moscow State University, Department of Soil Science, Moscow, Russia*

**e-mail: adrits@mail.ru*

***e-mail: klyuyvitkin@ocean.ru*

Received April 6, 2020; revised April 6, 2020; accepted April 8, 2020

Abstract—We studied sedimentation processes in the Lofoten Basin of the Norwegian Sea based on data of the Automatic Deep-Sea Sedimentation Observatory (ADSO) deployed for a year (August 2017–July 2018). The article presents estimates of the vertical fluxes of total sedimentary material, organic carbon (C_{org}), calcium carbonate ($CaCO_3$), biogenic silica (SiO_{2bio}), aluminum, and the particles of planktonic origin (pteropods, foraminifera, fecal pellets, necrozooplankton). The seasonal pattern of total vertical flux is characterized by a unimodal distribution with a maximum in September 2017 ($191 \text{ mg dry weight m}^{-2} \text{ day}^{-1}$) in the 0–500 m surface water layer. The total flux decreases markedly from November and reaches the minimum ($2.6 \text{ mg m}^{-2} \text{ day}^{-1}$) in March–April 2018. The maximum C_{org} flux values ($5.2 \text{ mg C m}^{-2} \text{ day}^{-1}$), $CaCO_3$ ($178 \text{ mg } CaCO_3 \text{ m}^{-2} \text{ day}^{-1}$), and SiO_{2bio} ($9.1 \text{ mg } SiO_{2bio} \text{ m}^{-2} \text{ day}^{-1}$) are observed in autumn. The value of fluxes and the portion of lithogenic material in it are higher at a depth of 2950 m due to redeposition from the nepheloid layer. The amplitude of flux variations during the year is noticeably smaller at this depth. The highest fluxes are related to the mass sedimentation of juvenile pteropods *Limacina retroversa*. The contribution of pteropods to vertical fluxes in autumn is 60–100% for $CaCO_3$ and 56–73% for C_{org} . The contribution of foraminifera to the total $CaCO_3$ flux does not exceed 6% and only reaches 60% at a depth of 550 m in October. The flux of fecal pellets, where ostracod pellets dominate, varies from <0.01 to $2.1 \text{ mgC m}^{-2} \text{ day}^{-1}$, making up from 0.1 to 90% of the C_{org} flux. The flux of zooplankton carcasses (ZCs) in the 0–550 m water layer varies from 0 to $0.45 \text{ mgC m}^{-2} \text{ day}^{-1}$, reaching the maximum value in February. The share of ZCs flux was 0–33% in the summer–autumn season, 12–52% in winter, and 23–41% in spring relative to the total (taking into account the ZCs) C_{org} flux. The ZCs flux varied from 0.04 to $0.22 \text{ mgC m}^{-2} \text{ day}^{-1}$ in the near-bottom water layer and amounted to 0.7–2% of the total C_{org} flux. The total contribution of all studied planktonic particles to the annual $CaCO_3$ flux was 16–47%, and their contribution to the annual C_{org} flux was 37–45%. Comparative analysis of our results and published data obtained in the 1990s demonstrates that the observed climatic changes (increasing temperature and salinity, as well as an increase in the thickness of the Atlantic water layer) in the Lofoten Basin did not result in significant changes in the quantitative characteristics of sedimentation process.

Keywords: sedimentation, vertical fluxes, organic carbon, calcium carbonate, biogenic silica, pteropods, foraminifera, fecal pellets, necrozooplankton, subarctic North Atlantic, climate change

DOI: 10.1134/S0001437020040074

INTRODUCTION

The study of sedimentary material, beginning from its formation to deposition on the bottom, is the most important task of modern sedimentology. Dispersed sedimentary material suspended in ocean waters with a thickness of many kilometers is the material from which bottom sediments and sedimentary rocks are formed [8]. Fluxes of sedimentary material in the ocean are one of the main quantitative sedimentation

parameters. They make it possible to study the dynamics of sedimentation processes, to analyze the transformation of sedimentary material during migration through the water column, and to evaluate the amount and composition of matter accumulated on the bottom. According to the biosedimentation concept of the living ocean [2, 9], sedimentary material which transported to the ocean from various sources (river runoff, aerosols, and endogenous matter), is transformed under the effect of marine biota. Living organ-

isms form vertical sedimentary material fluxes in seas and oceans and are the most important participants of sedimentation processes. The quantitative characterization of these processes, which control vertical transportation of suspended particulate matter (SPM), is of primary importance for understanding the global carbon cycle in the ocean and modern sedimentation processes. Studies of the annual flux and composition of sedimentary material is of particular interest, because they can give an idea not only about the seasonal variability of sedimentation processes, but also of the seasonal dynamics of the structure and functioning of epipelagic ecosystems.

The Norwegian Sea is a transit zone, through which warm and saline Atlantic water (AW) is transported from the North Atlantic to the Arctic Ocean [31, 48, 55]. The Lofoten Basin is the main heat reservoir of the Subarctic seas and, at the same time, an energy-active zone that directly affects the climate in Europe and further flow of AW into the Barents Sea and Fram Strait [41, 59].

A significant number of studies are devoted to sedimentation processes and mechanisms in this area [22, 30, 39, 44, 52, 60]. Most of them were performed in the 1980s–1990s. However, since the early 2000s, the flow of AW to the Arctic Ocean increases, which favors heat transfer through the Norwegian Sea to the north and northeast [38, 46]. The Norwegian Sea is characterized by a tendency toward an increase in water temperature, both in the surface and deeper layers, due to increasing heat content of the AW [42]. Modern data on fluxes and composition of sedimentary material and their seasonal variability are necessary to assess the possible impact of climate change on the quantitative parameters of sedimentation processes in this area.

Therefore, the aim of our study was investigation of vertical fluxes of the sedimentary material in the Lofoten Basin based on data obtained using Automatic Deep-Sea Sedimentation Observatory (ADSO) deployed during a year.

MATERIALS AND METHODS OF THE RESEARCHES

The data for the study were obtained in the Lofoten Basin in the course of a year, from July 22, 2017 (cruise 68 of the R/V *Akademik Mstislav Keldysh* [6]) to July 17, 2018 (cruise 71 of the R/V *Akademik Mstislav Keldysh* [13]), using the Automatic Deep-Sea Sedimentation Observatory (ADSO [10, 11]) (Fig. 1).

Hydrological data and water sampling. An SBE911p/SBE-32 profiling complex with 24 10-L Niskin bottles and temperature, conductivity, pressure, and turbidity sensors was used to study the water column during mooring and raising of the ADSO.

We collected 13 SPM samples. Samples were filtered under 400 mbar vacuum through membrane filters (pore size 0.45 μm and filter diameter 47 mm).

The SPM concentration was determined by weighing the filters with an accuracy of ± 0.01 mg. To determine the chlorophyll *a* (chl *a*) concentration, water samples were filtered through precombusted (at a temperature of 450°C) Whatman GF/F fiberglass filters under vacuum of no more than 200 mbar. The chl *a* concentration was determined by the fluorometric method (with extraction in 90% acetone) on a Trilogy 1.1 fluorometer (Turner Designs, United States) in the laboratory using the method described in [15]. The device was calibrated using the chl *a* standard of the Sigma company (C6144–1MG).

Sampling of sedimentary material. Sedimentary material was sampled by sediment traps at two depths: 550 m to assess the flux from the upper quasi-homogeneous AW layer; and 2950 m to evaluate the flux reaching the bottom and participating in sediment formation. The deposited material was taken by LOTOS-3 12-cup conical sediment traps with a sampling area of 0.5 m² (produced by the Experimental Design Bureau of Oceanological Engineering, Russian Academy of Sciences) programmed for a temporal resolution of 30 days.

The bottle samplers of the traps were filled with HgCl₂ solution (1% saturated solution) to avoid biological transformation of the sampled material. The salinity of the fixing solution was increased by adding NaCl to twofold the salinity of seawater (~70 PSU) to prevent leaching of the fixing solution from the samplers. Each trap sample was prefiltered through a sieve with a mesh size of 1 mm. Particles >1 mm retained by the sieve were placed in a separate bottle. A subsample of 30 mL was taken to analyze the composition of the trap material under a binocular microscope. A subsample of 100 ml was filtered through precombusted at a temperature of 450°C Whatman GF/F glass fiber filters to determine the total (C_{total}), organic (C_{org}), and carbonate (C_{carb}) carbon. The rest of the sample was filtered similarly to the SPM samples to determine the total fluxes and for subsequent material composition analysis.

Analysis of sedimentary material. Total Si and Al were determined by the photometric method according to the method of the Vernadskii Institute of Geochemistry and Analytical Chemistry, Russian Academy of Sciences, [3] modified by A.B. Isaeva (Shirshov Institute of Oceanology, Russian Academy of Sciences, IO RAS) to analyze small weighted portions of matter (accuracy 2–5%). Biogenic silica (SiO_{2bio}) was determined by the terrigenous matrix method as the difference between the contents of total and lithogenic silica.

Total and organic carbon was determined by high-temperature combustion with recording of released CO₂ by the automated coulometric method on an AN 7529 carbon analyzer (Russia) before and after acidification by 1 N HCl (accuracy 5–10%). The C_{carb} content was evaluated as the difference between C_{total} and

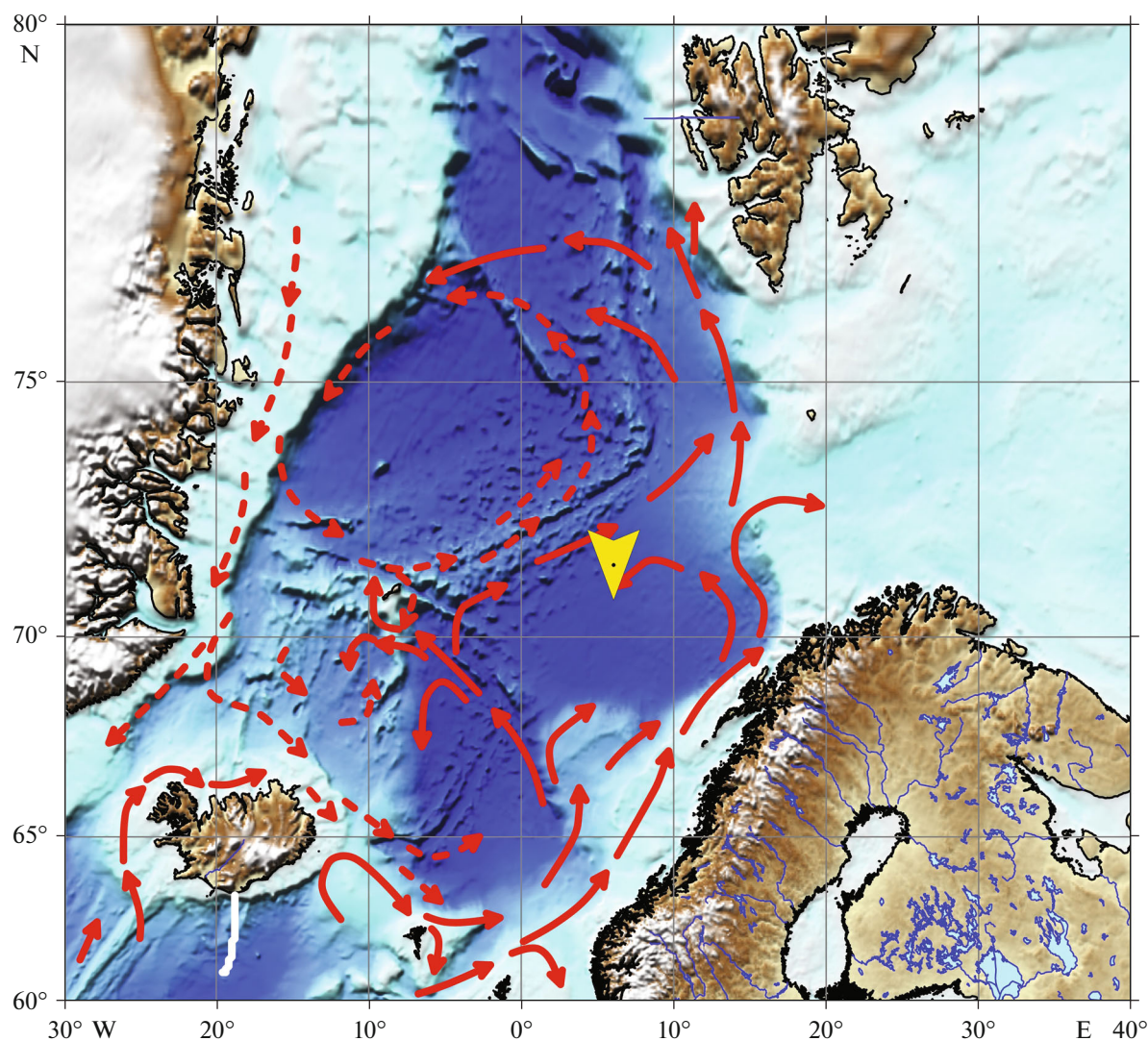


Fig. 1. Location of ADSO (station 5522), 71°33.773' N and 06°04.864' E, at a depth of 3000 m, on sketch map of subpolar North Atlantic. Arrows show general circulation of surface water [21].

C_{org} . The CaCO_3 content was calculated using the stoichiometric equation $100/12 \times C_{\text{carb}}$.

The micromorphology and composition of deposited matter were studied with a TESCAN VEGA 3 scanning electron microscope with an Oxford INCA Energy 350 microprobe attachment.

The chlorophyll concentration in the sea surface layer during the ADSO deployment was calculated using the Ocean Color Web search engine (<https://oceancolor.gsfc.nasa.gov/>) and SeaSAS 7.5.3 software (<https://seadas.gsfc.nasa.gov/>). Data of the MODIS-Aqua [54] LAC (Local Area Coverage) satellite scanner of the 3rd level (Level 3) were averaged for 20×20 and 50×50 km squares.

Analysis of the components of planktonic origin. The microscopic examination of sediment samples obtained after prefiltration through a 1 mm sieve showed that

shells of pelagic *Limacina retroversa* and planktonic foraminifera, as well as fecal pellets (FP) were the most numerous components of the fraction <1 mm. In addition, radiolarians of the order Spumellaria, eggs of planktonic animals, and objects, in appearance and size resembled the squid spermatophores ((Fig. 2) hereinafter, spermatophores) [37], were revealed in some samples.

The number and diameter of shells of *Limacina retroversa* and foraminifera were measured under a Leica binocular microscope at a magnification of $\times 100$ in the entire sample or in 1/10–1/200 portion of the sample (depending on the number of shells). Pellets were counted in a 1/10 portion of the sample and classified. The count in subsamples was performed in three replications. To estimate the content 100–200 pellets, 3–5 radiolarians, 2–3 spermatophores, and 30–50 eggs were randomly taken from the sample and thrice



Fig. 2. Photograph of objects from trap material identified as squid spermatophores.

washed with distilled water and filtered through a pre-combusted GF/F filter of 25 mm in diameter. The organic carbon content was determined with a Shimadzu TOC-VCPH analyzer.

To assess the content of organic and inorganic carbon in *Limacina*, we randomly selected 100–300 shells from samples with their high number, washed them three times in distilled water, and filtered through pre-combusted GF/F filter of 25 mm in diameter. The content of total and organic carbon was measured on a Shimadzu TOC-VCPH analyzer prior to and after acidification by 1N HCl. The content of inorganic (carbonate) carbon was calculated as the difference between C_{total} and C_{org} . The similar method was used to measure these parameters in foraminifera 0.2–0.4 mm in diameter. In small foraminifera (diameter <0.1 mm), only C_{total} was measured. The content of organic and inorganic carbon in these foraminifera was calculated based on the C_{org}/C_{total} and C_{carb}/C_{total} ratios obtained for larger shells.

The abundance and species composition of zooplankton carcasses (ZCs) were determined by examination of the entire sample > 1 mm under a Leica binocular microscope.

Only representatives with well-pronounced decomposition of body tissues and their detachment from the chitinous exoskeleton were taken into account [4]. To determine the organic carbon content of ZCs 1–5 ind of each species were selected, washed in distilled water, and placed on a precombusted GF/F filter. C_{org}

was determined with a Shimadzu TOC-VCPH analyzer.

Sampling of bottom sediments. Samples of bottom sediments were taken by a Mini Muc K/MT 410, KUM GmbH multicorer (Germany). The upper layer of the sample was used for preparations of standard slides, using the smear-slide method. Slides were studied onboard the research vessel under a Lomo POLAM L-213M polarizing microscope with an MS-5 camera (USB 2.0). Smear-slide is a thin layer (smear) of uncemented sediment fixed on the slide, using an optical liquid (Canadian balsam with a refractive index of $n = 1.55$). Smear-slide is a reliable rapid method for semi-quantitative diagnostics of mineral and particle-size composition of sediments, as well as of the determination of micro(nano)fossils. The study of smear-slides provides data on the composition of sediments [12]. The carbonate content in sediments was determined by an express-method based on measuring $CO_2 \uparrow$ pressure during the reaction of HCl with calcium carbonate, using a calcimeter.

RESULTS

Hydrological Conditions and the Concentration of SPM and Chlorophyll a

The vertical distribution of temperature, salinity, SPM concentration, and chl *a* in the water column at station 5522 is shown in Fig. 3.

The relatively warm and saline AW occupied the upper 0–625–695 m layer in the Lofoten Basin. The salinity of this layer ranged from 34.95 to 35.13 PSU.

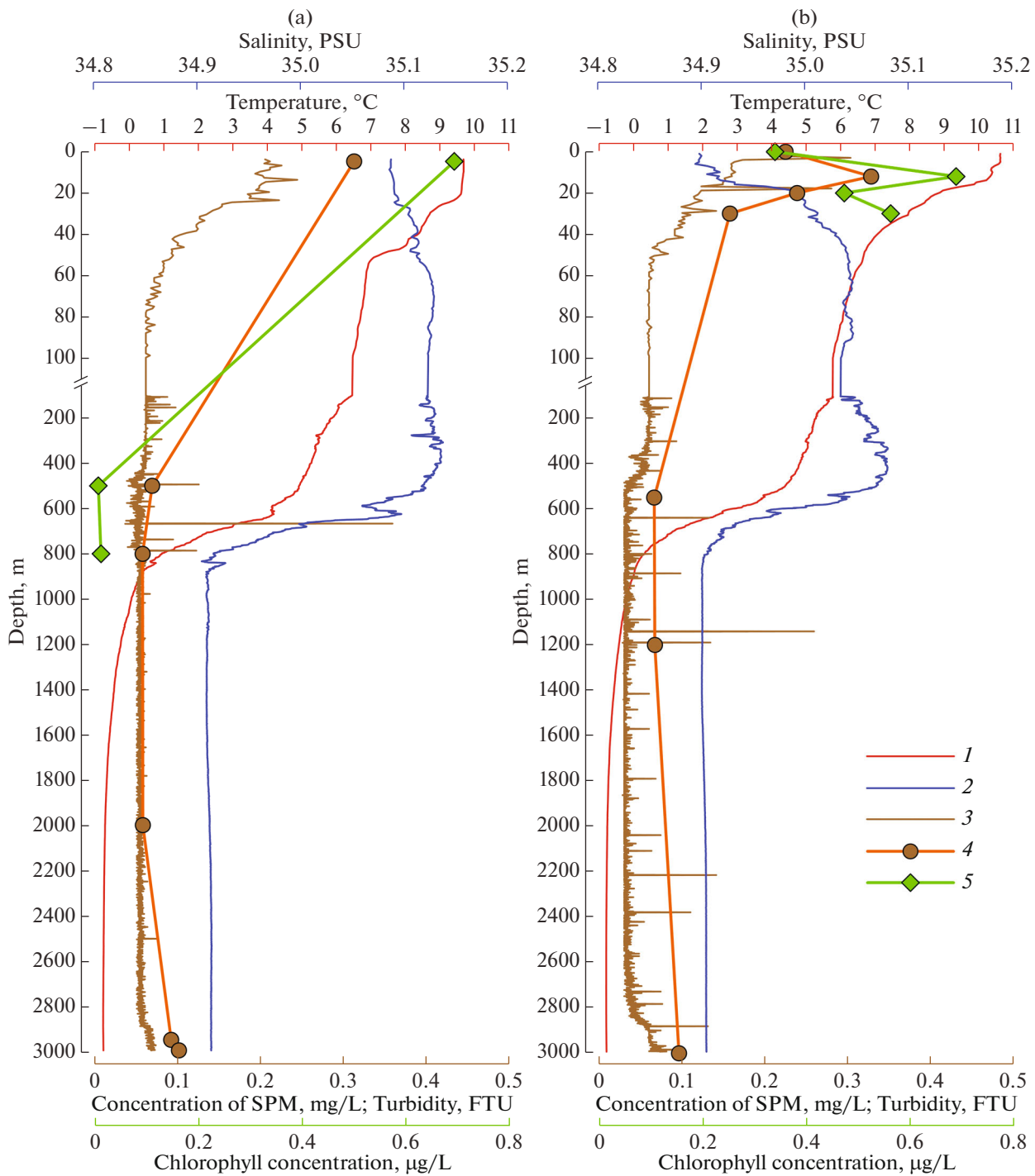


Fig. 3. Vertical distribution pattern of parameters of medium (temperature, salinity, oxygen content, and turbidity) based on CTD-sounding data and concentrations of SPM and chl *a* at ADSO at the time of setting (a) and raising (b) of traps. (1) Temperature; (2) salinity; (3) turbidity; (4) SPM concentration; (5) chlorophyll concentration.

The subsurface (0–20 m layer) was usually slightly desalinized, which was more pronounced in August 2018 (to 34.9 PSU). In the 0–50 m layer, a seasonal thermocline was seen in the both years, but it was less pronounced in August 2018. Water temperature in the upper desalinized layer reached 10.7°C in August 2018

and was by about 1°C lower in July 2017. In general, the temperature of the AW mass in the studied period varied from 9.7–10.7°C near the surface to 2.0°C at the boundary with the cold transitional water mass. We considered $\sigma = 27.9 \text{ kgm}^{-3}$ as the lower AW boundary according to [56].

The deep water mass occupied a layer from 625–695 m to the bottom. The water temperature here drop below zero (to -0.76°C), and the salinity was about 34.9 PSU (Fig. 3). The maximum density in the bottom layer was 28.08 kg/m^3 .

The concentration of SPM in the 0–5 m layer was 0.31 mgL^{-1} in July 2017 and 0.23 mg/L in August 2018. The chl *a* concentration varied from 0.69 to $0.34 \text{ }\mu\text{gL}^{-1}$, respectively. A subsurface maximum of SPM was recorded in August 2018 (0.33 mg L^{-1} at a depth of 15 m), which coincided with the maximum of chl *a* ($0.69 \text{ }\mu\text{gL}^{-1}$).

The concentration of SPM decreased several times with the depth and increased in the bottom nepheloid layer. The thickness of the nepheloid layer according to the data of CTD probes using a nephelometer varied from 150 m in July 2017 to 350 m in August 2018 (Fig. 3).

Analysis of satellite data showed that the chlorophyll concentration in the surface water layer of the Lofoten Basin was maximum at the end of summer and autumn 2017 (Fig. 4) and was significantly lower in autumn 2018.

Total Sedimentary Material Flux

Analysis of the trap material showed significant seasonal variability in the total matter fluxes in the subsurface layer (550 m depth) and relative uniformity in the near-bottom layer (2950 m depth) (Fig. 4).

In the subsurface layer, the seasonal pattern of the total flux was characterized by a unimodal distribution with the maximum in September 2017 ($191 \text{ mg m}^{-2} \text{ day}^{-1}$). Beginning from November, the flux decreased, reaching the minimum ($2.6 \text{ mg m}^{-2} \text{ day}^{-1}$) in March–April 2018. From May to July, the flux increased from 7.0 to $12.9 \text{ mg m}^{-2} \text{ day}^{-1}$.

In the bottom layer, the variability of fluxes during the year was less pronounced as compared to the subsurface layer. The flux in the bottom layer was the smallest ($107 \text{ mg m}^{-2} \text{ day}^{-1}$) in April, which coincides with the minimum flux in the subsurface layer.

Flux of Main Biogenic Components

SEM study of the samples revealed a great number of large (to $700 \text{ }\mu\text{m}$) shells of pteropods *Limacina retroversa* in the sedimentary material in August–October (Fig. 5). During these months, the CaCO_3 flux in the subsurface layer was high, with the maximum ($178 \text{ mg m}^{-2} \text{ day}^{-1}$) in September (Fig. 4). In this period, the CaCO_3 flux made up more than 90% of the total flux. During the rest of the year, it varied from 0.3 to $9.3 \text{ mg m}^{-2} \text{ day}^{-1}$. In the bottom layer, the maximum CaCO_3 flux was also in September ($240 \text{ mg m}^{-2} \text{ day}^{-1}$) and remained rather high (to $129 \text{ mg m}^{-2} \text{ day}^{-1}$) from August to February.

The C_{org} flux in the subsurface layer was the highest ($2.0\text{--}5.2 \text{ mg m}^{-2} \text{ day}^{-1}$) in August–October (Fig. 4). In the rest of the year, it did not exceed $1\text{--}2 \text{ mg m}^{-2} \text{ day}^{-1}$. In the bottom layer, it varied from 3.8 to $7.2 \text{ mg m}^{-2} \text{ day}^{-1}$ throughout the year.

The $\text{SiO}_{2\text{bio}}$ flux in the subsurface layer was highest ($9.1 \text{ mg m}^{-2} \text{ day}^{-1}$) in October. During the rest of the year, it did not exceed $2.7 \text{ mg m}^{-2} \text{ day}^{-1}$. In the bottom layer, the $\text{SiO}_{2\text{bio}}$ flux was significantly higher and varied throughout the year from 14.5 to $45.0 \text{ mg m}^{-2} \text{ day}^{-1}$.

The Si/Al ratio in the subsurface layer varied within 5.0–6.2 during the most part of the year, increasing sharply in October (to 20.9) and May–July (13.2–34.6). The enrichment of sedimentary material in total Si in relation to Al indicated an increase in the portion of biogenic Si in the flux. The Si content in the sedimentary material of the near-bottom layer (12.4–19.9%) was similar to its mean content in bottom sediments of the ocean (19.6% [7]). The Si / Al ratio in the bottom layer was 3.1–4.0, which was close to the mean ratio between these elements in the earth crust [49, 61]. The Si/Al ratio increased to 4.9 only in July, resulting in a slight enrichment of sedimentary material in the near-bottom layer with biogenic Si.

Sedimentation of the Components of Planktonic Origin

Pteropods *Limacina retroversa*. The entire *Limacina* population revealed in the trap material was represented by juvenile animals with a mean shell diameter of $0.49 \pm 0.19 \text{ mm}$ (at 550 m) and $0.48 \pm 0.12 \text{ mm}$ (at 2950 m). Almost all the shells were empty or with a small amount of organic matter. The seasonal sedimentation dynamics of these pteropods was characterized by a pronounced maximum ($13000\text{--}15000 \text{ shells m}^{-2} \text{ day}^{-1}$) in September at 550 m depth and in September–October at 2950 m (Fig. 6). In November, the vertical flux of pteropods sharply decreased and was almost zero in the rest of the year.

Planktonic foraminifera. Foraminifera were dominated by small ($<0.1 \text{ mm}$) shells; the share of larger ones ($0.2\text{--}0.4 \text{ mm}$) did not exceed 5%. Seasonal variation in the flux of these organisms during the year was unimodal with the maximum in October–November (Fig. 6). During winter months, foraminifera were only revealed in deep trap samples.

Fecal pellets (FP). Two different forms of faecal pellets were distinguished in the trap samples. The ovoid pellets were most abundant; a significant number of filiform pellets were only found in September–October in traps samples at 550 m depth (Fig. 6). The highest flux of FP in the upper 550 m layer ($900\text{--}2000 \text{ pellets m}^{-2} \text{ day}^{-1}$) was recorded at the end of the productive season. In the rest of the year, the flux was almost by an order of magnitude lower and did not exceed $200 \text{ pellets m}^{-2} \text{ day}^{-1}$. In the near-m layer, the minimum FP flux ($200\text{--}300 \text{ pellets m}^{-2} \text{ day}^{-1}$) was

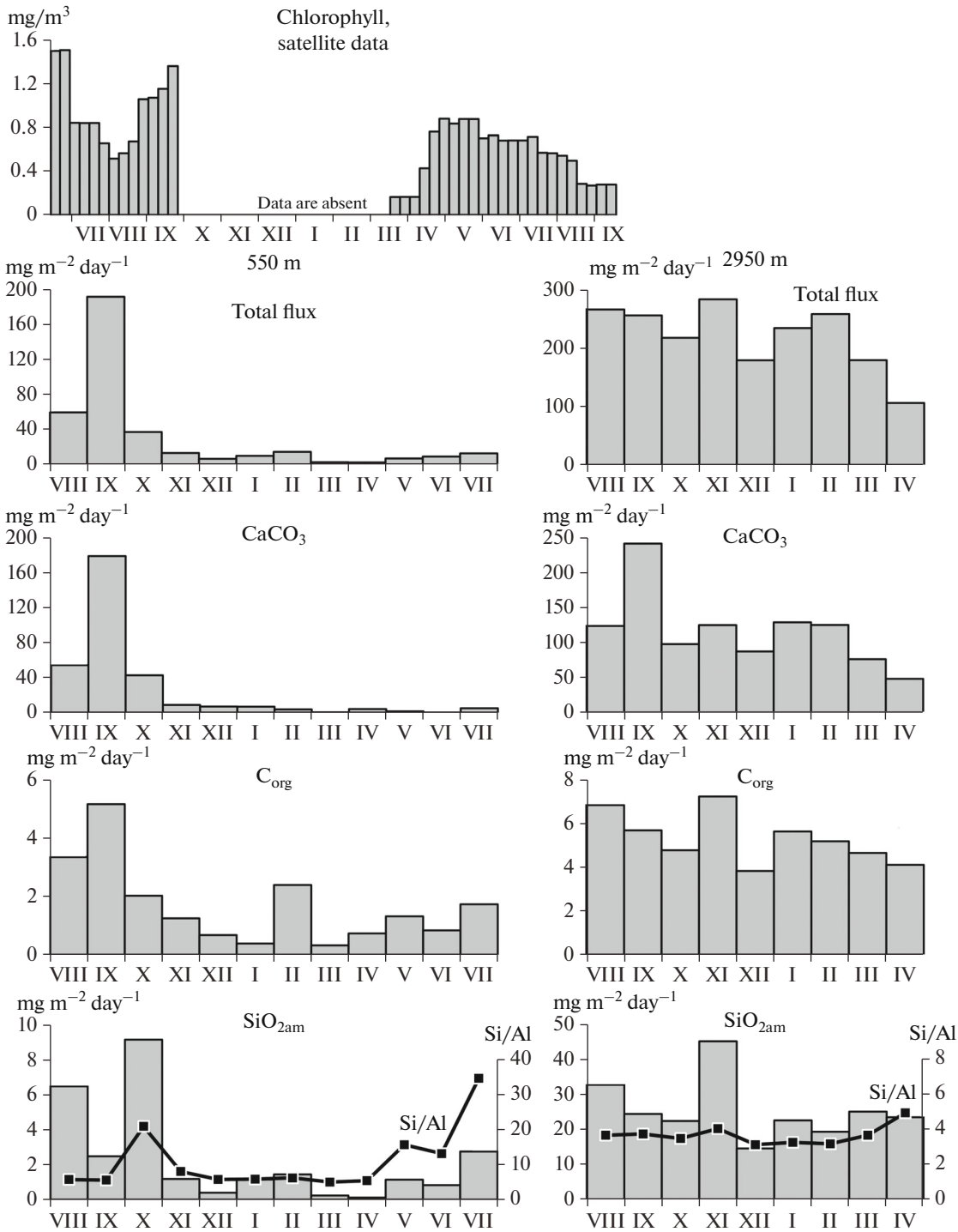


Fig. 4. Seasonal variability of chlorophyll concentration in surface layer, in vertical fluxes of total sedimentary material, calcium carbonate (CaCO_3), organic carbon (C_{org}), and amorphous silica ($\text{SiO}_{2\text{am}}$). Si/Al is ratio of total silica to aluminum in sedimentary material.

seen in December and March, and in the rest of the year, it varied from 1500 to 3500 pellets $\text{m}^{-2} \text{day}^{-1}$.

Eggs of planktonic animals were found only in samples of traps at 550 m in spring and summer. The maximum flux in May–June was 21–23 eggs $\text{m}^{-2} \text{day}^{-1}$.

Data on C_{org} and C_{carb} content of the described planktonic components of sedimentary material are given in Table 1.

Seasonal variations in the C_{org} and CaCO_3 flux related to sedimentation of different components are

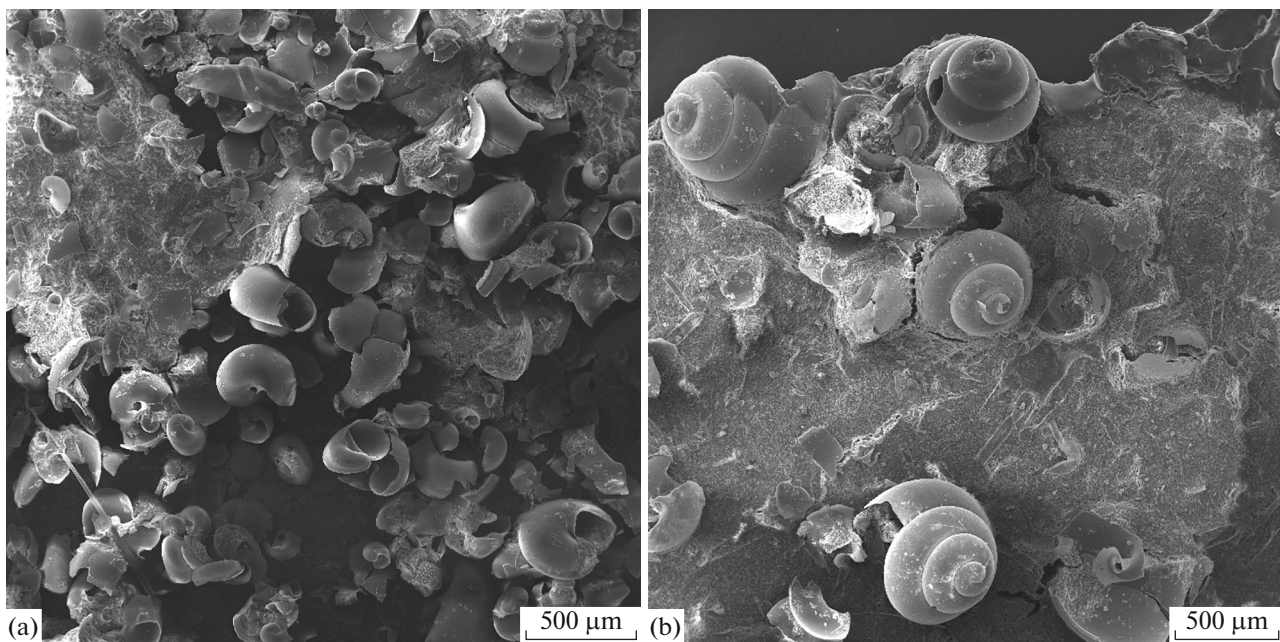


Fig. 5. Microphotographs of trap material in August, illustrating dominance of tests of *Limacina retroversa*: (a) 550 m horizon and (b) 2950 m horizon.

shown in Fig. 7. The highest C_{org} fluxes ($2.2\text{--}4.4 \text{ mgC m}^{-2} \text{ day}^{-1}$) in the 0–550 m layer occurred in late summer–autumn period. It was dominated by pteropods and FP ($1.1 \text{ mgC}_{\text{org}} \text{ m}^{-2} \text{ day}^{-1}$ for each) in August, by pteropods ($3.6 \text{ mgC m}^{-2} \text{ day}^{-1}$) in September, and by FP ($1.9 \text{ mgC}_{\text{org}} \text{ m}^{-2} \text{ day}^{-1}$) in October. In the other seasons, the C_{org} flux of the components of planktonic origin in this layer was much lower ($0.001\text{--}0.4 \text{ mgC}_{\text{org}} \text{ m}^{-2} \text{ day}^{-1}$). The contribution of all components to the total C_{org} flux was maximum in late summer and autumn, reaching 100% in October. The contribution to the total C_{org} flux did not exceed 1% in January–March, increased to 22% in April due to eggs sedimentation, dropped to 1% in June, and rose again to 12% in July. Seasonal variations of C_{org} flux at 2950 m

depth were similar to those described for the upper layer with high values ($2.4\text{--}5.2 \text{ mgC}_{\text{org}} \text{ m}^{-2} \text{ day}^{-1}$) in September–October and a significant decrease in other months. It was mainly determined by pteropods in autumn and by FP in the rest of year. The total contribution of these components to the total C_{org} flux varied from 80–100% in August–September to 4–35% in winter and spring.

The CaCO_3 flux in the entire water column was mainly determined by the pteropod sedimentation and varied from <1 to $104 \text{ mg m}^{-2} \text{ day}^{-1}$ (Fig. 7). The maximum values were obtained in September–October. At this time, from 40 to 100% of the total flux of calcium carbonate was determined by the sedimentation of *Limacina retroversa* shells. The contribution of fora-

Table 1. The content of total (C_{total}), organic (C_{org}), and carbonate (C_{carb}) carbon ($\mu\text{g}/\text{individual}$) in different components of sedimentary material

	C_{total}	C_{org}	C_{carb}
Limacina	1.07 ± 0.52 (6)	0.24 ± 0.09 (3)	0.83
Foraminifera <0.1 mm	0.028 ± 0.010 (9)	0.0078	0.02
Foraminifera 0.2–0.4 mm	0.14 ± 0.08 (3)	0.04	0.10
Oval pellets		0.48 ± 0.12 (6)	
Threadlike pellets		1.34	
Eggs 0.25 mm		1.65 ± 0.09 (2)	
Eggs 0.5 mm		7.46	

The data include mean \pm SD and the number of measurements in brackets.

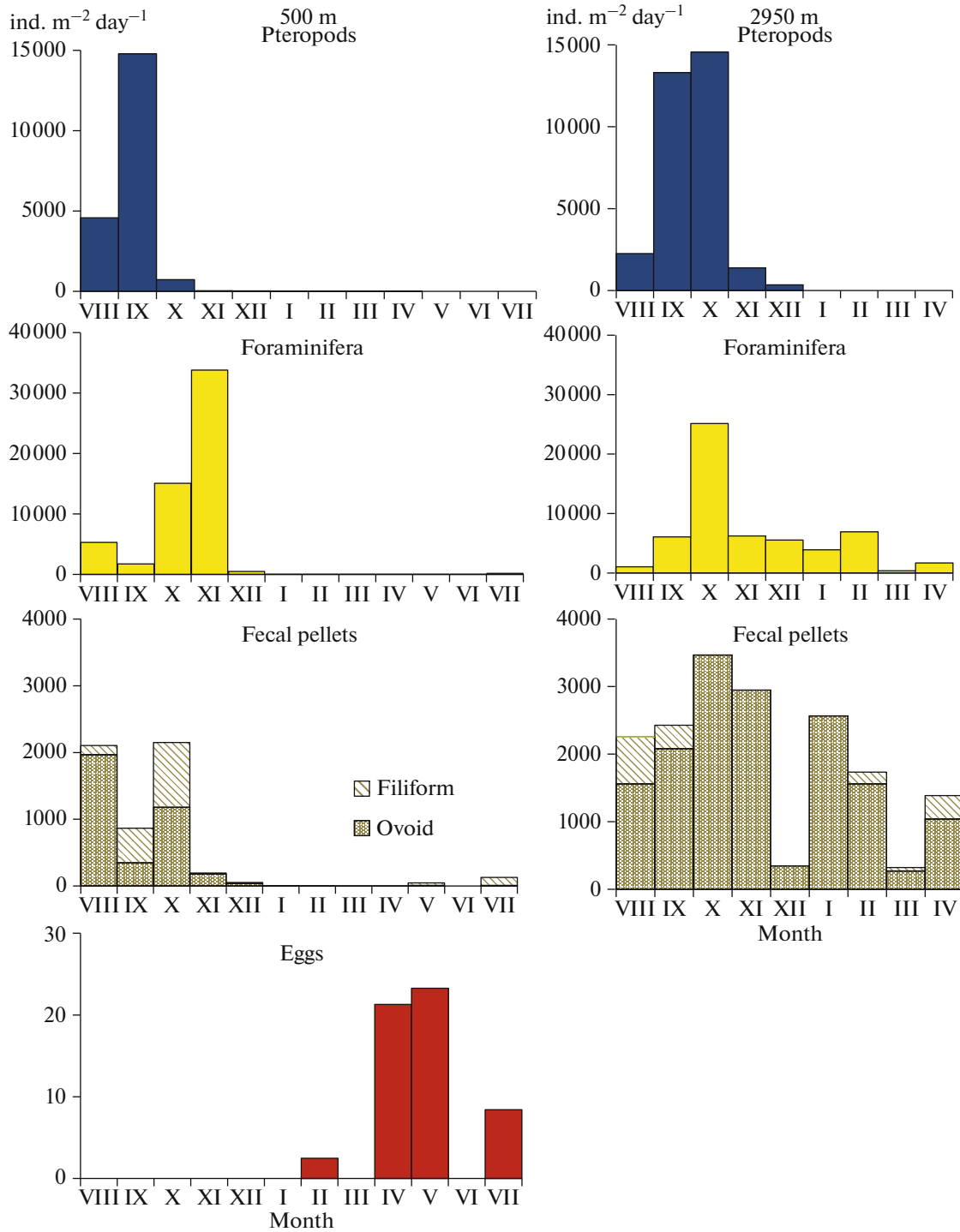


Fig. 6. Seasonal variability of vertical fluxes of different planktonic components (from microscopical countings).

minifera to the total CaCO₃ flux did not exceed 6%, and reached 60% only in October at 550 m depth.

Zooplankton carcasses. The amount and composition of ZCs in the trap samples varied significantly at different depths (Fig. 8). In traps at 500 m, copepods *Metridia longa* were the most abundant throughout the year, and there was a high number of deep-water cope-

pods *Heterorhabdus norvegicus* and *Paraeuchaeta* sp. in some periods. At 2950 m depth, copepods *Gaetanus* sp. were found only in three samples. The flux of these copepods was 0.3, 1.7, and 1.3 ind. m⁻² day⁻¹ in October, November, and January, respectively. In addition, radiolaria of the order Spumellaria was found in two samples (their flux was 3.4 and 3.9 ind. m⁻² day⁻¹ in

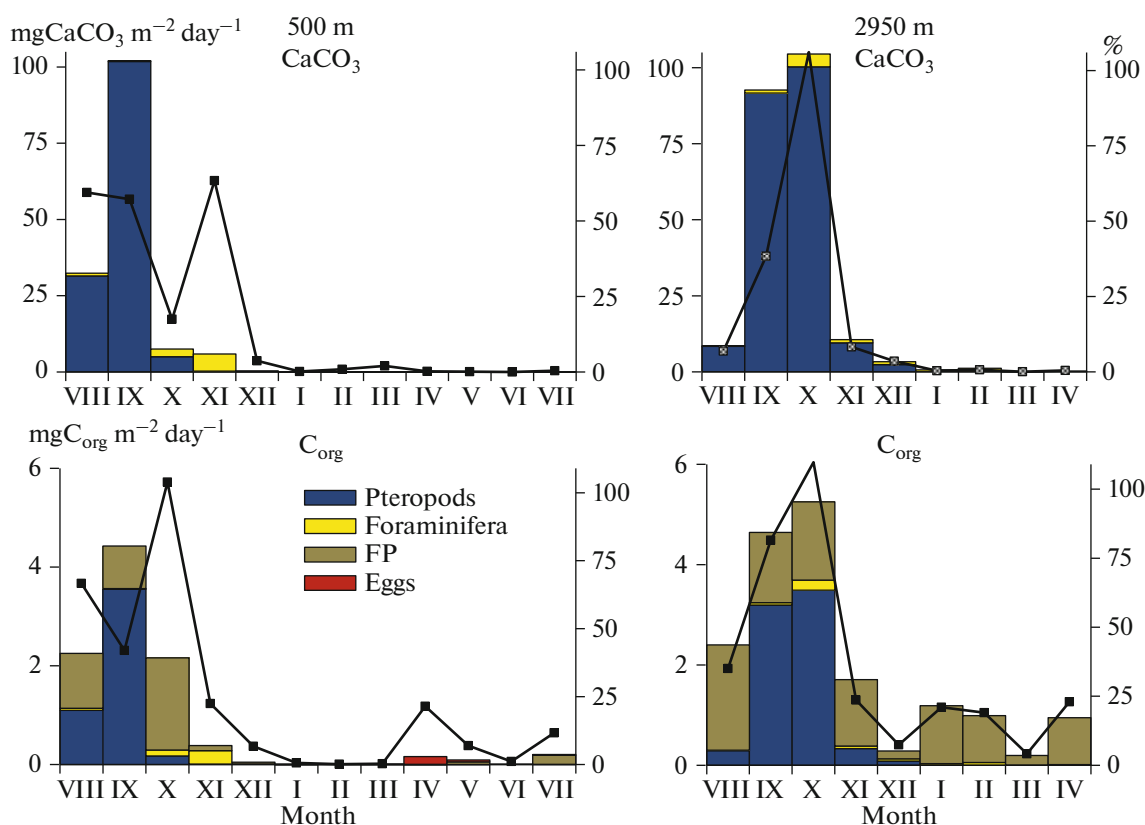


Fig. 7. Seasonal variability of C_{org} and $CaCO_3$ fluxes related to sedimentation of different planktonic components (columns) and their total contribution to C_{org} and $CaCO_3$ flux (line).

January and April, respectively) and spermatophores of squids in one sample in February (the flux was $1.2 \text{ ind. m}^{-2} \text{ day}^{-1}$). The C_{org} flux in the 0–550 m layer, calculated taking into account the data on the organic carbon content in ZCs (Table 2), varied from 0 to $0.45 \text{ mgC}_{org} \text{ m}^{-2} \text{ day}^{-1}$ with the maximum in February (Fig. 9). The contribution of different species depended on the season: more than half the total flux was related to sedimentation of dead *Paraeuchaeta* sp. in November–December, of *Amphipoda* in January–March, and *M. longa* in April–May. The contribution of ZCs to the total (including ZCs) C_{org} flux was 0–33% in summer and autumn, 12–52% in winter, and 23–41% in spring.

The C_{org} flux of ZCs in the near-bottom layer calculated taking into account the C_{org} content in *Gaetanus* sp ($139.5 \pm 23.0 \text{ mgC}_{org}/\text{ind.}$, $n = 3$), radiolaria ($8.4 \pm 7.2 \text{ mgC}_{org}/\text{ind.}$, $n = 3$), and spermatophores ($46.1 \pm 3 \text{ mgC}_{org}/\text{ind.}$, $n = 3$) varied from 0.04 to $0.22 \text{ mgC}_{org} \text{ m}^{-2} \text{ day}^{-1}$, which was 0.7–2% of the C_{org} flux (Fig. 9).

Biogenic components in bottom sediments. The exposed layer of Holocene sediments (0–26 cm) was represented by carbonate ($CaCO_3$ was more than 30% of wt) pelitic ooze with the content of the pelitic

fraction ($<0.01 \text{ mm}$) to ~80%. The upper layer (0–10 cm) of sediments was dominated (more than 80%) by the remains of planktonic and benthic organisms: foraminifera, coccoliths, diatoms, radiolaria, and sponge spicules. Microfossils revealed in the sediment were absolutely dominated (~65%) by coccolithophorides, foraminifera comprised 10–15%. Coccolithophorids were dominated by two species: large-cell *Coccolithus pelagicus* and small-cell *Emiliania huxleyi*. It should be pointed out that pteropods and their fragments were not found in the sediment samples, despite the dominance of these organisms in SPM in the water column.

DISCUSSION

The Lofoten Basin plays an important role in maintaining global meridional circulation in the region, where Atlantic water mass transfers heat to the atmosphere, is mixed with surrounding waters, and is transformed to form deep waters in the neighboring Greenland Sea [1]. According to long-term observations [24], the effect of increased AW temperature in the period from 1993 to 2017 is the most pronounced in this area. Even under conditions of a decrease in AW inflow by 1 Sv during this period (the data of the Norwegian

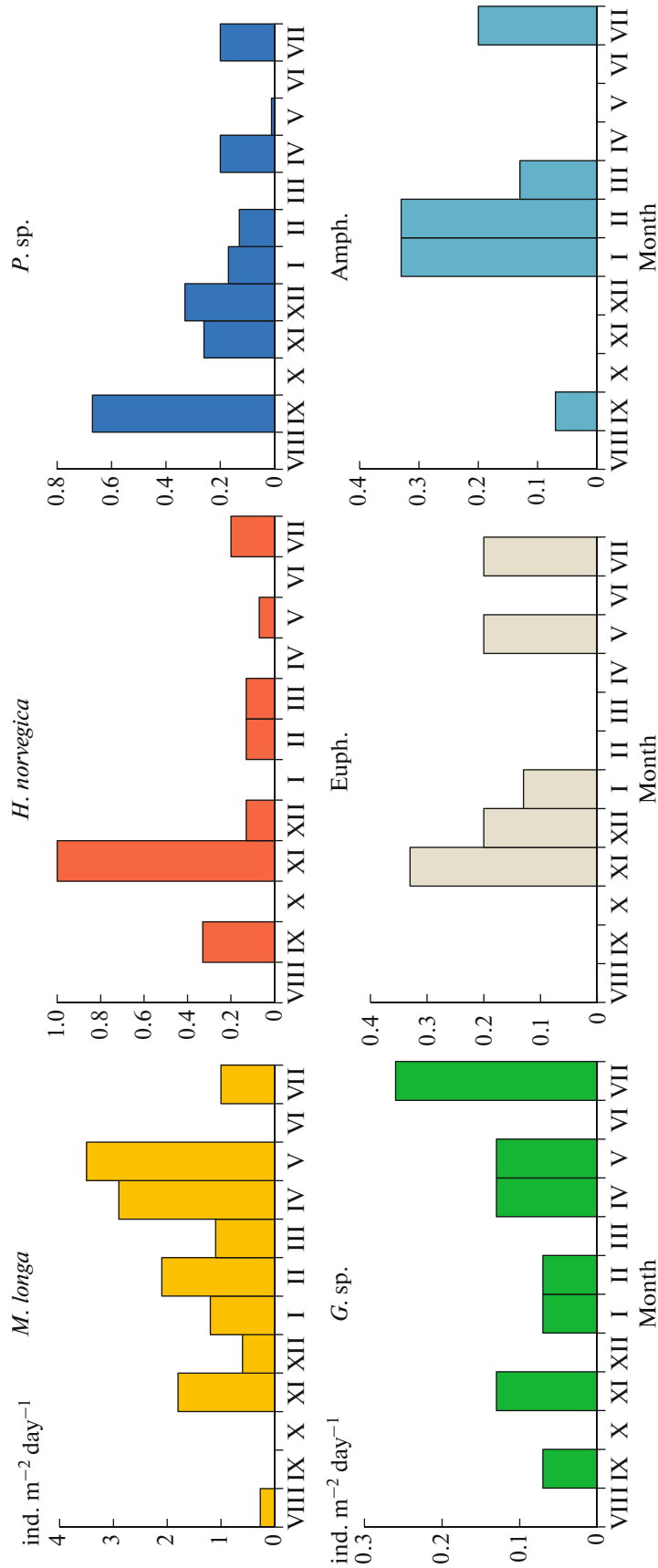


Fig. 8. Seasonal variability of vertical fluxes of different species of necrozooplankton at a depth of 550 m. M. longa—*Metridia longa*, H. norvegica—*Heterorhabdus norvegica*, P. sp.—*Paraeuchaeta* sp., G. sp.—*Gaetanus* sp., Euph.—*Euphausiidae*, and Amph.—*Amphipoda*.

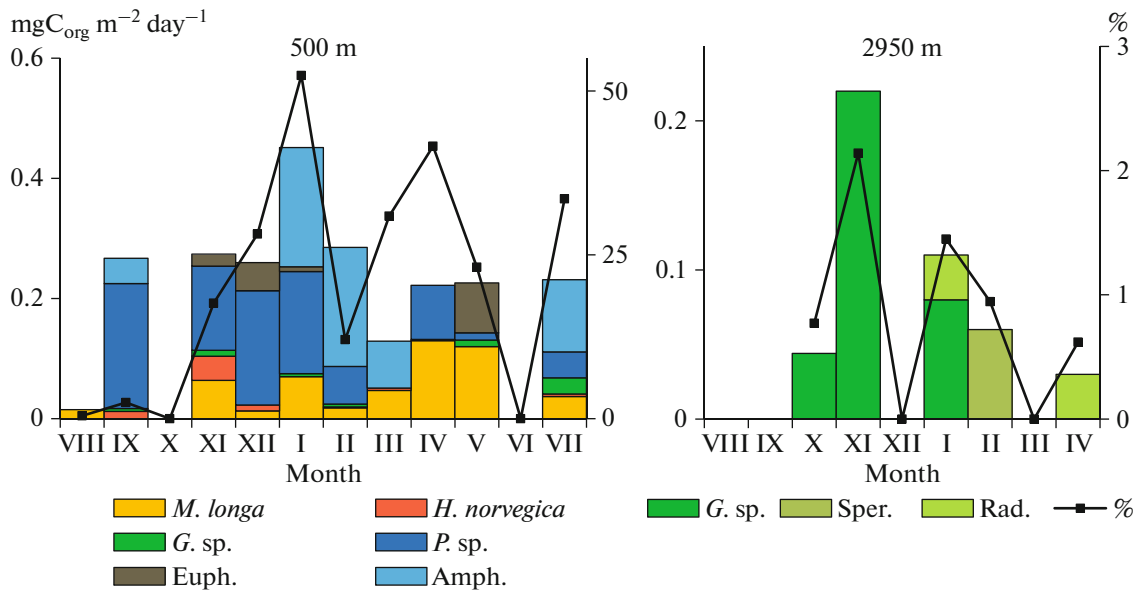


Fig. 9. Seasonal variability of C_{org} flux related to sedimentation of different species of necrozooplankton (columns) and their total contribution to C_{org} flux (line). *M. longa*—*Metridia longa*, *H. norvegica*—*Heterorhabdus norvegica*, *P. sp.*—*Paraeuchaeta sp.*, *G. sp.*—*Gaetanus sp.*, *Euph.*—*Euphausiidae*, *Amph.*—*Amphipoda*, *Rad.*—radiolaria, and *sper.*—spermatophores of squids.

Ocean Weather Station M, OWSM, 66° N, 2° E) [34], the thickness of the AW layer increased due to higher salinity and temperature of this layer [62].

To assess the effect of these changes on the parameters of sedimentation processes, we have compared our results with the data of annual sedimentation traps obtained in the Norwegian Sea and the Lofoten Basin in the 1980s–1990s (Table.3). Our estimates of the annual fluxes of the total sedimentary matter and C_{org}

at a depth of 550 m (11 g/m^2 and $0.8 \text{ gC}_{org}/\text{m}^2$) are 2–2.5 times lower than published data. These differences may be a result of interannual variability, which was pointed out in the previous studies [22, 44]. Another reason for the lower flux of sedimentary material and C_{org} in the period of our study may be lower AW inflow into the Norwegian Sea, resulting in a smaller amount of transported SPM. The differences are less pronounced in the bottom layer: according to our data, the

Table 2. The content of organic carbon ($\mu\text{gC}/\text{ind.}$) in different species of necrozooplankton

Month	<i>Metridia longa</i>		<i>Heterorhabdus norvegica</i>	<i>Gaetanus sp.</i>	<i>Paraeuchaeta sp.</i>	<i>Calanus sp.</i>	<i>Euphausiidae</i>			<i>Amphipoda</i>	
	females	males	females	females	females		CV	5–6 mm	9–10 mm	10–12 mm	12–14 mm
IX	–	–	36.5	–	312 ± 214 (3)	–	–	–	–	–	–
XI	44 ± 19 (2)	27 ± 5 (3)	40 ± 6 (3)	73 ± 32 (2)	689 ± 181 (2)	–	62 ± 13 (3)	–	–	–	–
XII	84	24 ± 2 (2)	73	–	565 ± 27 (3)	–	61	326	–	–	–
I	42 ± 3 (3)	23 ± 5 (3)	–	–	468 ± 50 (3)	–	–	–	–	–	567 ± 235 (4)
II	40 ± 6 (2)	14 ± 3 (4)	12	–	313 ± 96 (2)	–	–	–	–	–	–
III	55 ± 7 (3)	20	–	31	–	–	–	–	–	–	770
IV	72 ± 40 (2)	–	–	13	433 ± 191 (3)	30	–	–	–	–	724
V	54 ± 3 (3)	13 ± 4 (3)	–	82	182	70	–	–	419	–	–
VII	62 ± 10 (2)	19 ± 2 (2)	–	101 ± 20 (2)	215 ± 3 (2)	–	–	–	–	–	857 ± 126 (3)

The data include mean \pm SD and the number of measurements in brackets.

Table 3. Annual flux ($\text{g}/\text{m}^2/\text{year}$) of sedimentary material (total flux), suspended organic carbon (C_{org}), calcium carbonate (CaCO_3), and biogenic silica (Si_{bio}) in the Lofoten Basin according to data of annual sedimentation traps of 1983–1992

Trap depth	Year	Total flux	C_{org}	CaCO_3	Si_{bio}	Reference
2600 m	1983/1984	22.7	1.4	11.4	1.1	[35]
500 m	1988/1989	27.7	3.5	12.2	0.5	[44]
	1990/1991	20.0	1.7	6.3	0.5	
	1991/1992	16.9	1.5	7.6	0.3	
3000 m	1988/1989	57.6	2.7	15.1	0.8	[44]
	1990/1991	45.8	2.5	20.3	2.6	
	1991/1992	61.9	2.1	31.1	1.4	

annual flux of total sedimentary material was $79 \text{ g}/\text{m}^2$ and $23\text{--}62 \text{ g}/\text{m}^2$ according to [35, 44]; C_{org} flux was $1.9 \text{ gC}_{\text{org}}/\text{m}^2$ and $1.4\text{--}2.7 \text{ gC}_{\text{org}}/\text{m}^2$, respectively. The annual flux of CaCO_3 and SiO_2 is comparable to the values measured in the 1980s–1990s in the upper layer and is several times higher in the bottom layer.

A significant increase in the flux of sedimentary material and of all its components in the bottom layer was a specific feature of sedimentation processes in deep-water areas of the Norwegian Sea at the end of the last century [22, 23, 44]. The authors explained this phenomenon by the lateral advection and resuspension of SPM from the continental slope. According to their calculations, more than 50% of the total flux could not be explained by vertical sedimentation from the overlying layers and was related to redeposition of material from the nepheloid layer. The significant increase in the sedimentary material flux in combination with high turbidity in the bottom nepheloid layer ifound in our study also indicates to a significant role of the processes of resuspension and redeposition of SPM in the Lofoten Basin.

The seasonal pattern of vertical fluxes in the Lofoten Basin did not practically change over the period from 1988–1992 to 2017–2018: the maximum fluxes of sedimentary material, C_{org} , and CaCO_3 of the $<1 \text{ mm}$ fraction occurred in August–October according to [35, 44, 60] and in September according to our data (Fig. 4). The seasonal dynamics of vertical fluxes in earlier studies [44] was also the most pronounced at a depth of 500 m. In the near-bottom layer, the amplitude of changes in fluxes during the year was significantly smaller. According to [60], the shift of the seasonal maximum of the vertical flux to summer–autumn was typical for oceanic areas of the Norwegian Sea and was mainly related to mass sedimentation of pteropods *Limacina retroversa* [19, 39]. The flux of these organisms in the area of the Vøring Plateau (the Norwegian Sea) reached $8000 \text{ ind. m}^{-2} \text{ day}^{-1}$ in September [19]. According to calculations given in [17], their contribution to the annual CaCO_3 flux was 15%. In the Lofoten Basin, the maximum flux of *Limacina* in August–October 1983 comprised $150\text{--}550 \text{ ind. m}^{-2} \text{ day}^{-1}$ or

$8.4\text{--}18.4 \text{ mgCaCO}_3 \text{ m}^{-2} \text{ day}^{-1}$, and their contribution to CaCO_3 flux in that period was 15–24% or 11.5% of the annual flux [39]. According to our data, the maximum *Limacina retroversa* flux ($13000\text{--}15000 \text{ ind. m}^{-2} \text{ day}^{-1}$ or 60–100% of the CaCO_3 flux) was also observed in September–October, and the contribution of these animals to the annual CaCO_3 flux was 44 and 15% at depths of 550 and 2950 m, respectively. The contribution of *Limacina* to the annual C_{org} flux (11–18%) was close to the estimates (8% [17]) for the region of the Vøring Plateau. According to [39], the leading role of pteropods in the formation of the flux of biogenic material in autumn was determined by the mass mortality of juveniles, which appeared in the Norwegian Sea in August, and the high rate of their sedimentation ($1\text{--}2.5 \text{ cm}/\text{s}$ [26]). At this rate, dead *Limacina* could reach the bottom in just a few days. It is reasonable that according to our data, their number in the traps at the subsurface and near-bottom depths was almost equal. The results indicate that at the present time, pteropods also play a significant role in the vertical transportation of C_{org} and calcium carbonate in the Lofoten Basin. These data confirm the conclusions [17, 19, 20, 25], concerning a significant role of pteropods in the functioning of biological carbon pump and in the formation of the carbonate system in the Norwegian Sea and in some areas of the Arctic basin.

Planktonic foraminifera are a constant and numerous component of sedimentary material and play an important role in the vertical transportation of CaCO_3 [29, 33, 53]. The annual flux of CaCO_3 of foraminifera in different regions of the world ocean is $0.2\text{--}22 \text{ gCaCO}_3/\text{m}^2$, and its contribution to the CaCO_3 flux varies from 2 to 100% [53]. Our data ($0.3 \text{ gCaCO}_3/\text{m}^2/\text{year}$, 3% of the annual flux) are close to the minimum values typical for deep ocean. Fluxes in different seasons ($0.1\text{--}5.6 \text{ mgCaCO}_3 \text{ m}^{-2} \text{ day}^{-1}$) obtained in this study are within the range of $0.5\text{--}6.3 \text{ mgCaCO}_3 \text{ m}^{-2} \text{ day}^{-1}$ calculated for the Greenland and Norwegian seas in the layers deeper than 500 m [53], and their contribution to CaCO_3 fluxes could reach 60%.

Since the 1990s, there has been a general trend of increasing contribution of calcifying plankton to the vertical flux of sedimentary material in the North Atlantic, and, conversely, of a decreasing role of diatoms and other siliceous plankton [14]. The high solubility of aragonite shells of pteropods at greater depths as compared to calcite shells of foraminifera and coccolithophorids [20, 40] explains the absence of pteropod shells in bottom sediments of the Lofoten Basin. In the bottom sediments of the subpolar North Atlantic, shells of foraminifera and coccolithophorids are widely spread [5]. According to our data, the upper layer of bottom sediments in the Lofoten Basin is mainly represented by coccoliths. Similar data on the composition of bottom sediments in the Lofoten Basin are given in [52]. The vertical flux of coccolithophorids in the Lofoten Basin is more than $100 \times 10^6 \text{ m}^{-2} \text{ day}^{-1}$ [52]. The role of foraminifera in the vertical flux is insignificant.

Zooplanktonic FP are the most important component of the C_{org} flux [58]. According to the modern data, the contribution of FP to C_{org} flux in different regions of the world ocean varies from 1 to >90% [58]. It has been shown in recent years that a significant portion of FP produced in the upper productive layer is remineralized and does not reach deep layers [28, 43, 47, 63]. The accumulation of FP in intermediate and deep layers is related to the feeding of deep-sea zooplankton [36] or with diurnal vertical migrations of zooplankters [28]. We have not found copepods FP in the of trap samples in the Lofoten Basin. An insignificant contribution of copepods FP to C_{org} flux in layers deeper than 500 m in the Norwegian Sea is also pointed out in [18, 22]. Most of samples are dominated by ovoid FP. Their significant amount in the material of sediment traps in the region of the Vøring Plateau in the Norwegian Sea is also mentioned in [19]. According to the authors, the most likely source of these pellets are planktonic ostracods which are abundant in deep water layers. It is interesting that according to our data, the seasonal variability in the flux of ovoid FP in the near-bottom layer is less pronounced as compared to the upper 500 m layer. The annual flux of FP in the studied region increased with the depth from $0.13 \text{ g } C_{\text{org}}/\text{m}^2$ (500 m) to $0.40 \text{ g } C_{\text{org}}/\text{m}^2$ (2950 m), and their contribution to annual C_{org} flux was 16–21%. These results confirm the idea that in the intermediate and deep layers FP produced by deep-sea zooplankton play an important role in the vertical transport of organic matter.

The studies of ZCs flux in different regions of the World Ocean summarized in [57] show that it comprises a significant part of C_{org} flux in the coastal areas and over the continental shelf outside the period of phytoplankton blooming. According to our data, the ZCs flux in the Lofoten Basin varies from 0 to $0.45 \text{ mg } C_{\text{org}} \text{ m}^{-2} \text{ day}^{-1}$ with the maximum at 550 m depth in January. The ZCs flux during this month comprises 52% of the total C_{org} flux (C_{org} flux < 1 mm + the flux

of ZCs C_{org}). A significant increase in ZCs flux in winter is also shown for the Beaufort Sea and the Amundsen Bay [50, 51]. According to these authors, the contribution of ZCs in this season reaches 86–91% of the total C_{org} flux. The annual flux of ZCs C_{org} in the upper 70-m layer of the Beaufort Sea ($2.5 \text{ g } C_{\text{org}} \text{ m}^{-2}$) is more than 20 times higher than the flux ($0.11 \text{ g } C_{\text{org}} \text{ m}^{-2}$) calculated on the basis of our data for the 0–550-m layer. The annual ZCs C_{org} flux in the near-bottom layer decreased by an order of magnitude to $0.01 \text{ g } C_{\text{org}} \text{ m}^{-2}$. In shallow traps in the Beaufort Sea, in the Amundsen Gulf and in the Kara Sea older copepodite stages of *Calanus glacialis* dominate the ZCs flux [4, 50, 51]. In deep traps in the Lofoten Basin, the carcasses of *Calanus finmarchicus*, dominating zooplankton with respect to biomass in the Norwegian Sea, [27, 45], were only found (3 ind.) in one sample at a depth of 550 m. The absence of *Calanus* carcasses in the trap material throughout the year could be related to the vertical distribution pattern of this species at different stages of its life cycle. In spring and summer, when the population of *C. finmarchicus* in the Norwegian Sea is concentrated in the upper 100-m-thick layer [16], the flux of dead copepods does not reach the mesopelagic layers. From July to February, most of the population inhabits deep layers, where it survives winter in diapause [16]. According to [32], the overwintering part of the population is the most numerous in the 600–1300 m layer, i.e., deeper than the depth of the of the upper trap. It seems likely that during this period, carcasses of *C. finmarchicus* could not reach the bottom, being decomposed by bacteria or consumed by deep-sea zooplankters. It may be assumed that low flux of *Calanus* carcasses is one of the reasons of low ZCs fluxes in the deep-water areas of the Norwegian Sea as compared to the shallower Arctic seas. The dramatic decrease of ZCs flux in the near-bottom layer of the Lofoten Basin indicates the insignificant role of this component of sedimentary matter as a source of organic matter for deep-sea benthic communities.

CONCLUSIONS

Analysis of the results of our research and data obtained in the 1990s shows that the observed climatic changes (increased temperature, salinity, and thickness of the AW layer) in the Lofoten Basin of the Norwegian Sea did not result in significant changes in the quantitative parameters of the sedimentation process. In general, the pattern of seasonal changes in the vertical flux of sedimentary material and its main components is similar to those described in the publications about 30 years ago. The revealed differences in the total and C_{org} fluxes in the upper 500 m layer may be explained by interannual variability or a result of a decrease in the AW inflow to the Norwegian Sea observed in 1993–2017. Composition of components of planktonic origin in the sedimentary material and

their contribution to C_{org} and $CaCO_3$ fluxes significantly correspond to the previously obtained results. Similarly to the earlier studies, pteropods *Limacina retroversa* play a significant role in the vertical flux of C_{org} and calcium carbonate in the Lofoten Basin. They determine the carbon cycle in the water column, but they are not directly involved in sediment formation. The material from our traps was dominated by FP of ostracods, which was also indicated in earlier studies of the 1990s.

Estimation of the ZCs flux performed for the first time in the Norwegian Sea indicates the insignificant role of this component in vertical C_{org} transport to deep layers. One reason for the low ZCs flux in comparison with other Arctic seas may be the absence of carcasses of *Calanus finmarchicus*, which dominates zooplankton.

Our data show that the sedimentation process in deep-water areas of the Norwegian Sea is mainly controlled by zooplankton. All the studied planktonic components in total (pteropods, foraminifera, eggs, FP, and ZCs) contribute to the annual calcium carbonate flux by 16–47% and to the annual C_{org} flux by 37–45%.

ACKNOWLEDGMENTS

The authors are grateful to the crew of the R/V *Akademik Mstislav Keldysh*, A.I. Kochenkova, E.O. Zolotykh, A.V. Bulokhov, and G.V. Malafeev for their assistance in collecting and processing trap material samples, and also to D.V. Eroshenko and S.M. Isachenko for aid in sampling sedimentary material.

FUNDING

The field studies were supported by the state budget (financing of marine expeditions) and the Russian Science Foundation (project no. 14-50-00095). Geochemical and biological research was supported by the Russian Foundation for Basic Research (project nos. 18-05-60069 Arctic, 19-05-00787, and 19-05-00022). Processing of material was partially supported by the state task of the Ministry of Education and Science of the Russian Federation (topic no. 0149-2019-0007). Analysis of data and preparation of the published work were supported by the Russian Science Foundation (project no. 20-17-00157).

REFERENCES

1. T. V. Belonenko, A. V. Koldunov, E. V. Sentyabov, and A. L. Karsakov, "Thermohaline structure of the Lofoten vortex in the Norwegian Sea based on in-situ and model data," *Vestn. S.-Peterb. Gos. Univ., Nauki Zemle* **63** (4), 502–519 (2018).
2. M. E. Vinogradov and A. P. Lisitsyn, "Global pattern of the life distribution in the ocean and their reflection in the composition of bottom sediments: the distribution pattern of plankton and benthos in the ocean," *Izv. Akad. Nauk SSSR, Ser. Geol.*, No. 3, 5–25 (1981).
3. E. M. Gel'man and I. Z. Starobina, *Photometric Analysis of Rock-Forming Elements in Ores, Rocks, and Minerals* (Vernadsky Institute of Geochemistry and Analytical Chemistry, Academy of Sciences of USSR, Moscow, 1976) [in Russian].
4. A. V. Drits, M. D. Kravchishina, A. F. Pasternak, et al., "Role of zooplankton in the vertical mass flux in the Kara and Laptev seas in fall," *Oceanology (Engl. Transl.)* **57**, 841–854 (2017).
5. E. M. Emel'yanov, *Sedimentogenesis in the Atlantic Ocean Basin* (Nauka, Moscow, 1982) [in Russian].
6. M. D. Kravchishina, A. N. Novigatskii, A. S. Savvichev, et al., "Studies on sedimentary systems in the Barents Sea and Norwegian–Greenland basin during cruise 68 of the R/V *Akademik Mstislav Keldysh*," *Oceanology (Engl. Transl.)* **59**, 158–160 (2019).
7. A. P. Lisitsyn, *Ocean Sedimentation: Lithology and Geochemistry* (Nauka, Moscow, 1978) [in Russian].
8. A. P. Lisitsyn, "Modern concepts on sedimentation in the oceans and seas. Ocean as the natural chronicles of interaction of the Earth's geospheres," in *The World Ocean, Vol. 2: Physics, Chemistry, and Biology of the Ocean. Sedimentation in the Ocean and Interaction of the Earth's Geospheres*, Ed. by L. I. Lobkovskii and R. I. Nigmatulin (Nauchnyi Mir, Moscow, 2014), pp. 331–571.
9. A. P. Lisitsyn and M. E. Vinogradov, "Global pattern of the life distribution in the ocean and their reflection in the composition of bottom sediments: formation and distribution of biogenic sediments," *Izv. Akad. Nauk SSSR, Ser. Geol.*, No. 4, 5–24 (1982).
10. A. P. Lisitsyn, V. N. Lukashin, A. N. Novigatskii, et al., "Deep-water observatories in the Trans-Caspian cross section: continuous studies of scattered sedimentary matter," *Dokl. Earth Sci.* **456**, 709–713 (2014).
11. A. P. Lisitsyn, A. N. Novigatskii, V. P. Shevchenko, et al., "Dispersed organic matter and its fluxes in oceans and seas from the example of the White Sea: results of a 12-year study," *Dokl. Earth Sci.* **456**, 635–639 (2014).
12. A. P. Lisitsyn and V. P. Petelin, "Preliminary treatment of samples of marine sediments in the on-board conditions," *Tr. Inst. Okeanol. im. P.P. Shirshova, Akad. Nauk SSSR* **19**, 240–251 (1956).
13. A. N. Novigatsky, S. V. Gladyshev, A. A. Klyuvitkin, et al., "Multidisciplinary research in the North Atlantic and Arctic on cruise 71 of the R/V *Akademik Mstislav Keldysh*," *Oceanology (Engl. Transl.)* **59**, 464–466 (2019).
14. A. Antia, N. Koeve, W. Fischer, et al., "Basin-wide particulate carbon flux in the Atlantic Ocean: regional export patterns and potential for atmospheric CO_2 sequestration," *Global Biogeochem. Cycles* **15**, 845–862 (2001).
15. E. J. Arar and G. B. Collins, *Method 445.0. In vitro Determination of Chlorophyll "a" and Pheophytin "a" in Marine and Freshwater Algae by Fluorescence: Revision 1.2* (US Environmental Protection Agency, Washington, DC, 1997).
16. E. G. Arashkevich, K. S. Tande, A. F. Pasternak, and B. Ellertsen, "Seasonal moulting patterns and the generation cycle of *Calanus finmarchicus* in the NE Norwe-

- gian Sea, as inferred from gnathobase structures, and the size of gonads and oil sacs," *Mar. Biol.* **146** (1), 119–132 (2004).
17. U. V. Bathmann, T. T. Noji, and B. Bodungen, "Sedimentation of pteropods in the Norwegian Sea in autumn," *Deep-Sea Res., Part A* **38** (10), 1341–1360 (1991).
 18. U. V. Bathmann, T. T. Noji, M. Voss, and R. Peinert, "Copepod fecal pellets: abundance, sedimentation and content at a permanent station in the Norwegian Sea in May/June 1986," *Mar. Ecol.: Prog. Ser.* **38**, 45–51 (1987).
 19. U. V. Bathmann, R. Peinert, T. T. Noji, and B. V. Bodungen, "Pelagic origin and fate of sedimenting particles in the Norwegian Sea," *Prog. Oceanogr.* **24** (1–4), 117–125 (1990).
 20. E. Bauerfeind, E.-M. Nöthig, B. Pauls, et al., "Variability in pteropod sedimentation and corresponding aragonite flux at the Arctic deep-sea long-term observatory HAUSGARTEN in the eastern Fram Strait from 2000 to 2009," *J. Mar. Syst.* **132**, 95–105 (2014).
 21. J. Blindheim and F. Rey, "Water-mass formation and distribution in the Nordic Seas during the 1990s," *ICES J. Mar. Sci.* **61**, 846–863 (2004).
 22. B. Bodungen, A. Antia, E. Bauerfeind, et al., "Pelagic processes and vertical flux of particles: an overview of a long-term comparative study in the Norwegian Sea and Greenland Sea," *Geol. Rundsch.* **84**, 11–27 (1995).
 23. B. Bodungen, U. Bathmann, M. Voss, and M. Wunsch, "Vertical particle flux in the Norwegian Sea—resuspension and interannual variability," in *Proceedings of the Symposium on Sediment Traps in Marine Ecological Research and Monitoring "Sediment Trap Studies in the Nordic Countries," Fiskebäckskil, Sweden, 1990*, Ed. by P. Wassmann, et al. (NurmiPrint Oy, Nurmijärvi, 1991), Vol. 2, pp. 116–136.
 24. S. Broomé, L. Chafik, and J. Nilsson, "Mechanisms of the time-varying sea surface height and heat content trends in the eastern Nordic seas," *Ocean Sci. Discuss.*, (2019).
<https://doi.org/10.5194/os-2019-109>
 25. K. Busch, E. Bauerfeind, and E.-M. Nöthig, "Pteropod sedimentation patterns in different water depths observed with moored sediment traps over a 4-year period at the LTER station HAUSGARTEN in eastern Fram Strait," *Polar Biol.* **38** (6), 845–859 (2015).
 26. R. H. Byrne, J. G. Acker, P. R. Betzer, R. A. Feely, and M. H. Cates, "Water column dissolution of aragonite in the Pacific Ocean," *Nature* **312** (5992), 321–326 (1984).
 27. J. Carstensen, A. Weydmann, A. Olszewska, and S. Kwaśniewski, "Effects of environmental conditions on the biomass of *Calanus* spp. in the Nordic seas," *J. Plankton Res.* **34** (11), 951–966 (2012).
 28. E. L. Cavan, F. A. Le Moigne, A. J. Poulton, et al., "Attenuation of particulate organic carbon flux in the Scotia Sea, Southern Ocean, is controlled by zooplankton fecal pellets," *Geophys. Res. Lett.* **42** (3), 821–830 (2015).
 29. N. Chernihovsky, A. Torfstein, and A. Almogi-Labin, "Seasonal flux patterns of planktonic foraminifera in a deep, oligotrophic, marginal sea: sediment trap time series from the Gulf of Aqaba, northern Red Sea," *Deep Sea Res., Part I* **140**, 78–94 (2018).
 30. G. Dall'Olmo and K. A. Mork, "Carbon export by small particles in the Norwegian Sea," *Geophys. Res. Lett.* **41**, 2921–2927 (2014).
 31. J. Dugstad, I. Fer, J. LaCasce, et al., "Lateral heat transport in the Lofoten Basin: near-surface pathways and subsurface exchange," *J. Geophys. Res.: Oceans* **124** (5), 2992–3006 (2019).
 32. A. Edvardsen, J. M. Pedersen, D. Slagstad, et al., "Distribution of overwintering *Calanus* in the north Norwegian Sea," *Ocean. Sci.* **2**, 87–96 (2006).
 33. N. O. Eguchi, H. Kawahata, and A. Taira, "Seasonal response of planktonic foraminifera to surface ocean condition: sediment trap results from the central North Pacific Ocean," *J. Oceanogr.* **55** (6), 681–691 (1999).
 34. T. Eldevik, B. Risebrobakken, A. Bjune, et al., "A brief history of climate in the northern seas from the Last Glacial Maximum to global warming," *Quat. Sci. Rev.* **106**, 225–246 (2014).
 35. S. Honjo, S. J. Manganini, and G. Wefer, "Annual particle flux and a winter outburst of sedimentation in the northern Norwegian Sea," *Deep-Sea Res., Part A* **35** (8), 1223–1234 (1988).
 36. S. Honjo, S. J. Manganini, R. A. Krishfield, and R. Francois, "Particulate organic carbon fluxes to the ocean interior and factors controlling the biological pump: a synthesis of global sediment trap programs since 1983," *Prog. Oceanogr.* **76**, 217–285 (2008).
 37. H.-J. T. Hoving, J. A. A. Perez, and K. S. R. Bolstad, "The study of deep-sea cephalopods," *Adv. Mar. Biol.* **67**, 235–359 (2014).
 38. S. Lind, R. B. Ingvaldsen, and T. Furevik, "Arctic warming hotspot in the northern Barents Sea linked to declining sea-ice import," *Nat. Clim. Change* **8**, 634–639 (2018).
 39. G. Meinecke and G. Wefer, "Seasonal pteropod sedimentation in the Norwegian Sea," *Palaeogeogr., Palaeoclimatol., Palaeoecol.* **79** (1–2), 129–147 (1990).
 40. A. Mucci, "The solubility of calcite and aragonite in seawater at various salinities, temperatures, and one atmosphere total pressure," *Am. J. Sci.* **283** (7), 780–799 (1983).
 41. J. E. Ø. Nilsen and E. Falck, "Variations of mixed layer properties in the Norwegian Sea for the period 1948–1999," *Prog. Oceanogr.* **70** (1), 58–90 (2006).
 42. "Norwegian Sea ecoregion: ecosystem overview," in *ICES Ecosystem Overviews. Norwegian Sea Ecoregion* (International Council for the Exploration of the Sea, Copenhagen, 2017), Chap. 12.1, pp. 1–15.
 43. K. Olli, C. W. Wexels Riser, P. Wassmann, et al., "Seasonal variation in vertical flux of biogenic matter in the marginal ice zone and the central Barents Sea," *J. Mar. Syst.* **38** (1–2), 189–204 (2002).
 44. R. Peinert, A. Antia, E. Bauerfeind, et al., "Particle flux variability in the Polar and Atlantic biogeochemical provinces of the Nordic Seas," in *The Northern North Atlantic: A Changing Environment*, Ed. by P. Schafer, (Springer-Verlag, Berlin, 2001), pp. 53–68.
 45. B. Planque and S. D. Batten, "*Calanus finmarchicus* in the North Atlantic: the year of *Calanus* in the context of

- interdecadal change,” *ICES J. Mar. Sci.* **57** (6), 1528–1535 (2000).
46. I. V. Polyakov, A. V. Pnyushkov, M. B. Alkire, et al., “Greater role for Atlantic inflows on sea-ice loss in the Eurasian Basin of the Arctic Ocean,” *Science* **365** (6335), 285–291 (2017).
 47. M. Reigstad, C. W. Wexels Riser, P. Wassmann, and T. Ratkova, “Vertical export of particulate organic carbon: attenuation, composition and loss rates in the northern Barents Sea,” *Deep Sea Res., Part II* **55** (20–21), 2308–2319 (2008).
 48. T. Rossby, M. D. Prater, and H. Søyland, “Pathways of inflow and dispersion of warm waters in the Nordic seas,” *J. Geophys. Res.: Oceans* **114**, C04011 (2009).
 49. R. L. Rudnick and S. Gao, “Composition of the continental crust,” in *Treatise on Geochemistry*, Vol. 4: *The Crust* (Elsevier, Amsterdam, 2014), Chap. 4.1, pp. 1–51.
 50. M. Sampei, H. Sasaki, H. Hattori, et al., “Significant contribution of passively sinking copepods to the downward export flux in Arctic waters,” *Limnol. Oceanogr.* **54**, 1894–1900 (2009).
 51. M. Sampei, H. Sasaki, A. Forest, and L. Fortier, “A substantial export flux of particulate organic carbon linked to sinking dead copepods during winter 2007–2008 in the Amundsen Gulf (southeastern Beaufort Sea, Arctic Ocean),” *Limnol. Oceanogr.* **57** (1), 90–96 (2012).
 52. C. Samtleben and T. Bickert, “Coccoliths in sediment traps from the Norwegian Sea,” *Mar. Micropaleontol.* **16** (1–2), 39–64 (1990).
 53. R. Schiebel, “Planktic foraminiferal sedimentation and the marine calcite budget,” *Global Biogeochem. Cycles* **16** (4), 13–1–13–21 (2002).
 54. SeaWiFS project, NASA/Goddard Space Flight Center and ORBIMAGE. <http://oceancolor.gsfc.nasa.gov>.
 55. O. H. Segtnan, T. Furevik, and A. D. Jenkins, “Heat and freshwater budgets of the Nordic seas computed from atmospheric reanalysis and ocean observations,” *J. Geophys. Res.: Oceans* **116**, C11003 (2011).
 56. Ø. Skagseth and K. A. Mork, “Heat content in the Norwegian Sea, 1995–2010,” *ICES J. Mar. Sci.* **69** (5), 826–832 (2012).
 57. K. W. Tang and D. T. Elliott, “Copepod carcasses: occurrence, fate and ecological importance,” in *Copepods: Diversity, Habitat and Behavior*, Ed. by L. Seuront (Nova Science, Hauppauge, 2014), pp. 255–278.
 58. J. T. Turner, “Zooplankton fecal pellets, marine snow, phytodetritus and the ocean’s biological pump,” *Prog. Oceanogr.* **130**, 205–248 (2015).
 59. D. L. Volkov, T. V. Belonenko, and V. R. Foux, “Puzzling over the dynamics of the Lofoten Basin—a sub-Arctic hot spot of ocean variability,” *Geophys. Res. Lett.* **40** (4), 738–743 (2013).
 60. P. Wassmann, R. Peinert, and V. Smetacek, “Patterns of production and sedimentation in the boreal and polar Northeast Atlantic,” *Polar Res.* **10** (1), 209–228 (1991).
 61. K. H. Wedepohl, “The composition of the continental crust,” *Geochim. Cosmochim. Acta* **59** (7), 1217–1232 (1995).
 62. N. Weidberg and S. L. Basedow, “Long-term variability in overwintering copepod populations in the Lofoten Basin: the role of the North Atlantic oscillation and trophic effects,” *Limnol. Oceanogr.* **64** (5), 2044–2058 (2019).
 63. C. W. Wexels Riser, P. Wassmann, K. Olli, et al., “Seasonal variation in production, retention and export of zooplankton faecal pellets in the marginal ice zone and central Barents Sea,” *J. Mar. Syst.* **38** (1–2), 175–188 (2002).

Translated by I. Bel’chenko